Mr. Manjunath Raikar. International Journal of Engineering Research and Applications
www.ijera.com
ISSN: 2248-9622, Vol. 9, Issue 4, April, 2019, pp: 94-100

RESEARCH ARTICLE OPEN ACCESS

A New Approach to High-Frequency Electrical Characterization in Magnetic Passive Devices

Mr. Manjunath Raikar
Lecturer / Department of Electrical & Electronics
Sri Channakeshava Govt Polytechnic - Bankapur-581202, Dist Haveri
manjunathraikarn@gmail.com

Date of Submission: 01-04-2019 Date of acceptance: 10-04-2019

ABSTRACT
The power supply on chip modules relies heavily on integrated magnetic components. These magnetic devices have low inductances and operate at very high frequencies due to the needs of the applications. Not all the necessary information about the magnetic device is provided by conventional small-signal measurements. To precisely test the performance of devices under actual operating settings, including nonlinear core effects, it is crucial to design novel setups to apply big signals. Since the excitation current can be configured through each winding—ac current up to 0.5 A at frequencies up to 120 MHz and dc bias current up to 2 A through one or both windings—the suggested experimental setup is appropriate to measure the device impedance under various large-signal test conditions, like those in the actual converter. Commercial instruments are used to measure voltage and current. Processing the voltage and current waveforms to determine the impedances requires accounting for the attenuation and delay caused by the probes and the experimental apparatus because of the high frequency of the test and the characteristics of the probes. This article describes the compensation test used to determine this attenuation and delay. Ultimately, the suggested configuration is verified by the measurement of a microfabricated, two-phase linked inducer on silicon.

Keywords: ***DC-DC Convertor, impedance measurement, integrated magnetic, large signal testing, thin-film indicators***

I. INTRODUCTION

The difficulty in distributing electricity has been brought to light by the constant push for electronic gadgets to become smaller, more useful, and more efficient effectively to these gadgets. A growing number of people believe that granular voltage regulation, or VR, might help multipurpose electronic devices meet their power needs. By positioning these granular VRs near the point-of-load, parasitic connection efficiency losses may be minimized. To do this, a power system in package or power system on chip is usually used, in which the VR is either packed or constructed monolithically with load [1]. In addition to better parasitic losses, this method offers enhanced dynamic responsiveness from the VR according to load needs. Furthermore, granular virtual reality systems employ multiphase topologies, wherein the utilization of phase shedding offers enhanced light load efficiency in contrast to single-phase topologies [2] – [6].

The most popular topology for integrated VR (IVR) is a buck type of dc–dc converter since it has more efficiency than linear and hybrid regulators and can execute step-down functions as needed by the applications as shown the figure of High Frequency Electrical Characterization Technique. Inductors are typically used in buck converter circuits to temporarily store electrical energy. To effectively store energy, these magnetic devices employ a soft magnetic material core. When compared to an air-core device without the soft magnetic core, the energy density of the inductor is much increased when soft magnetic cores are used [6]– [9]. Ferrite magnetic cores are used in traditional inductor topologies because of their inexpensive cost and extremely low power loss density. By using quicker switches and drivers, advanced power switching circuits lower the need for energy storage in these devices, allowing for the use of other thin-film soft magnetic materials as cores. Thin-film materials provide several advantages over lower saturation density ferrite-based devices, one of them being their greater saturation flux density, which allows for devices with a smaller volume and footprint. Furthermore, thin-film alloys may be manufactured using

microelectromechanical systems-based manufacturing processes on silicon substrates [7], enabling additional integration of these passive devices with other silicon-fabricated active components.

A great deal of work has gone into creating the right magnetic core for inductors that will be utilized in IVR applications [5] – [10]. But because they are far more conductive than ferrites, most soft magnetic thin films have larger losses than ferrites, especially when it comes to eddy current losses. Furthermore, while higher permeability of thin-film materials allows for miniaturization, a drawback of such permeability is that smaller devices' ability to handle current is limited by the shorter magnetic path length of the material when used in single-phase inductors. This problem is solved by using negatively linked phase inductors, which create opposing flux in the core and cause flux cancellation, allowing the cores to handle greater currents. Furthermore, the negatively linked phases lessen output ripple by reducing the summation of currents in various phases. Additionally, the energy is stored in the device's leakage inductance, allowing for a quicker transient reaction to the load.

As previously said, quicker switching circuits make it possible to employ soft magnetic thin films, and as a result, scientists are concentrating more on creating novel magnetic thin film alloys and device designs that can function at frequencies higher than 100 MHz, Because core losses are extremely nonlinear with respect to both frequency and B-field, empirical characterization—rather than modeling is the preferred approach for designing the component. This highlights how difficult it is to characterize these materials and devices at high frequencies. Network analyzers are frequently employed for high-frequency characterization; however, they only apply a tiny signal current, which means that the characterization only yields information on copper and core eddy current losses. It takes a large-signal characterization setup to assess coupled systems' loss performance with accuracy.

The complete core loss, including eddy current, hysteresis, and excess eddy current losses, is provided by the device impedance measurement since the large signal characterization circumstances are usually chosen to match those of the real converter. A large-signal measurement system's primary concerns are producing a sufficient excitation signal and developing a high-precision technique for measuring the equivalent impedance. Numerous publications on the large-signal characterization of discrete passive devices have been published [11]– [13]. However, the requirement for high-frequency characterization has made the work on integrated thin-film devices difficult. The large signal experiments carried out to characterize a device up to 120 MHz are presented in this study, faster transition to the and faster switching circuits and increasingly. The difficulties in obtaining precise voltage and current data at these frequencies and the difficulty of compensating for the probe lag are also covered in this work.

II. PROPOSED LARGE SIGNAL SETUP

The on-silicon coupled inductor's large-signal characterization is typically achieved by providing the proper excitation in one or two phases and monitoring the voltage and current to determine the inductor's impedance. Accurately extracting the voltage and current waveforms at very high frequencies is a major difficulty. The purpose of the proposed experimental setup, whose schematic is shown in Fig. 1, is to:

1) produce both ac and dc currents through one or both windings, simulating the conditions that the device would have on the actual converter.
2) increase the accuracy of the measurements at very high frequencies by using commercial probes to sense voltage and current.

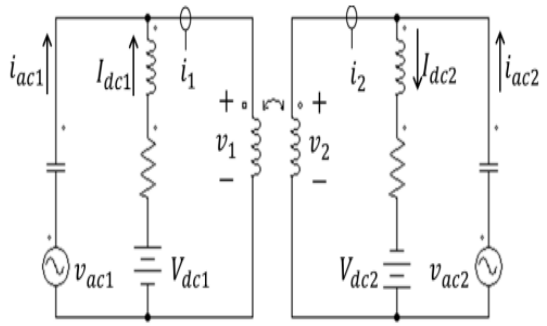

Figure No. 1: The large-signal testing circuit's schematic

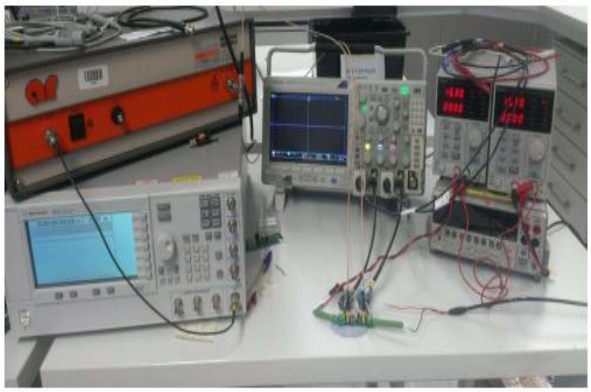

Figure No. 2: Large-Signal Setup

With the measurement of the voltage and current waveforms (v1, i1, v2, i2) and the applied voltages (vac1, Vdc1, Vdc2, vac2), as shown in Fig. 1, one may determine the mutual impedance or the self-impedance under various operating situations. As a result, v1 and i1 are used to compute the self-impedance of the primary winding Z11, while v2 and i1 are used to calculate the core-impedance Z12. The resistive component is the real portion of the impedance, while the inductive component is computed directly as the imaginary part of the impedance.

Figure 2 shows an image of the configuration. Every winding in Fig. 1 has two distinct branches linked in parallel to provide the excitation signals.

1. AC Signal Generation (Vac1 and Vac2): Through a SMA connection, an RF amplifier driven by a signal generator introduces ac current into the printed circuit board (PCB) circuit. A DC blocking capacitor is placed in series with the RF amplifier.
2. The process of creating DC current (Vdc1 and Vdc2) A power resistor limits the overall current, and an inductance blocks the ac current when an independent dc source is connected in series with it.

Applying ac current via both windings up to 120 MHz and dc bias current up to 2 A is possible with the intended arrangement, which is summed up in Table I. While the voltage and current are monitored with commercial probes, the data is acquired using a mixed domain oscilloscope.

1. ***Voltage Phase:*** The Tektronix TAP1500 voltage probes, which have an impedance of around 1 pF, were chosen for this application. It is essential to utilize high impedance probes for increased accuracy since the impedance of the probes might create an extra route for the current at high frequencies. There are reports on this problem in [14] - [15].
2. ***Current Phase:*** Due to its short latency and wide bandwidth (200 MHz), the Pearson Current Monitor model 2877 is chosen for the current measurements as opposed to using resistors, as is frequently documented in the literature [12]. There are no harmonics in the measured current that may cause the current probe to become nonlinear. It does, however, only work with ac current and reaches saturation at modest dc bias levels. The current monitor adjusts the dc current to prevent saturation. This compensation is depicted (main side) in the schematic in Figure 3. No ac current is anticipated in the dc branch, as the self-resonance of the dc choke is around 190 MHz (series inductance in Table I), which might contaminate the current measurement.

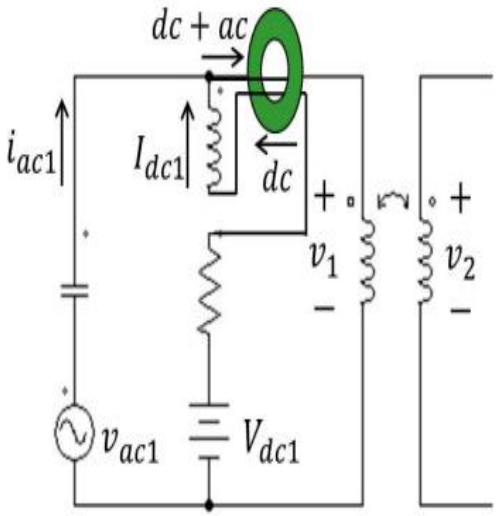

Figure No. 3: dc current compensation using current monitor to prevent saturation

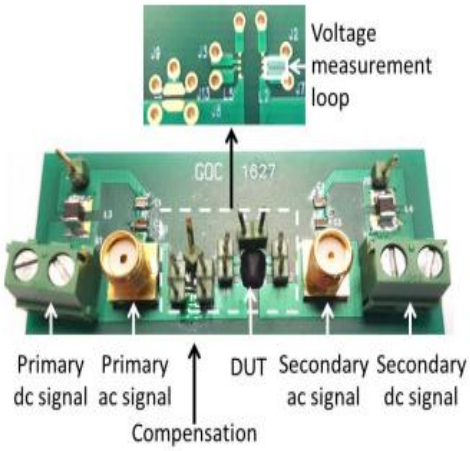

Figure No. 4: Large Signal Testing Circuit

The precision of the measurements may be impacted by a variety of problems [11]. The suggested technique is the primary cause of mistakes in this approach, which are as follows.

1. ***Circuit Parasitic***: The PCB was made with the least amount of circuit parasitic influence in mind. Figure 4 displays the intended PCB along with a detailed view of the device's connections. A 4-terminal Kelvin connection, with the driven current traces isolated from the voltage measurement traces, was used to monitor the voltage in the magnetic device's terminals. Since there is very little current flowing through the voltage measurement loop, AC mutual resistance shouldn't be an issue. Mutual inductance has the potential to generate voltage

in the measuring loop; nevertheless, to reduce the impact of parasitic on the voltage measurement, the voltage probes are connected as near to the device as feasible; this results in the smallest possible darkened region in Figure 4. Therefore, in this work, a mistake resulting from layout parasitic is deemed insignificant.

2. ***Probes***: Since the voltage and current waveforms are used directly to estimate the impedance, the probes themselves become the primary source of inaccuracy. Error in Amplitude: The current waveform may be attenuated due to the current monitors' amplitude response as a function of frequency. Measurement and consideration of this attenuation should be made while post-processing the waveforms.

3. ***Delay Between the Signals***: Because voltage and current probes each have a unique propagation delay, the current and voltage waveforms that the scope measures may be temporally skewed in relation to one another. This indicates that the data pairings are not time coincidence, hence a method for correcting the time skew in the waveform postprocessing must be included.

Based on the identified sources of error, a compensation test is necessary to reduce the influence of the probes on measurement accuracy. As a result, figuring out the measuring system's attenuation and the time interval between channels is the first step.

III. METHODOLOGY

In the compensation test, an impedance Z that is known at the test frequency is measured for both voltage across and current (Fig. 5). For the compensation test in this instance, a high-Q surface mounted device (SMD) with a 220-nF capacitance has been used (compensation block in Fig. 4). The Class 1 NP0 dielectric capacitor CC0402JRNPO9BN221 exhibits a low fluctuation in capacitance and equivalent series resistance with frequency. Using an E4990 Impedance Analyzer and Qc = tan (89.3°) = 81 at 100 MHz, it was tested in tiny signal. These results indicate that the capacitor at 100 MHz is near to being perfect. Additionally, when frequency increases, its impedance reduces, boosting current and improving the signal-to-noise ratio.

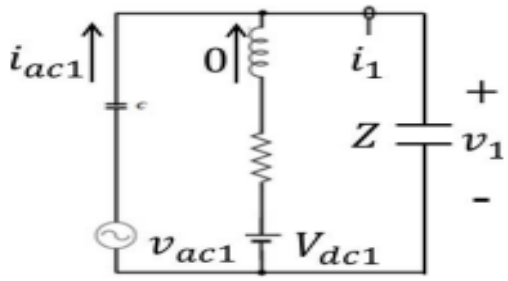

Figure No. 5: Schematic of the compensation test.

Calculated are the first harmonics, V1 and I1, of the observed voltage v1 and current i1. Subsequently, the voltage and current are computed using (1) and (2) to determine the attenuation and phase shift imposed by the probes and the measuring apparatus. These values are then compared to the theoretical ones. It is thus necessary to postprocess the recorded voltage and current waveforms to adjust for attenuation and to disked using the estimated attenuation and phase shift at every frequency to reliably determine any impedance using the suggested setup.

$$Attenuation = \frac{|I_1|Z||}{|V_1|}$$

$$Phase\ Shift = \angle V_1 - \angle I_1 - \angle Z_1$$

An understanding of the significance of the compensating test may be gained by looking at the 100 MHz waveforms in Figure 6. The continuous line representations of the waveforms match the signals measured during the compensation test. The phase shift between the observed voltage and current is seen to be entirely different from what would be predicted in a high-Q capacitor. The current postprocessed, including the phase shift and computed attenuation, is represented by the dotted line. Based on the technology being used, the observed delay is rather consistent with what would be predicted. The data sheets state that the voltage probe has a delay of 5.3 ns and the current monitor at 100 MHz has a delay of around 0.2 ns (6°), however they do not give tolerances.

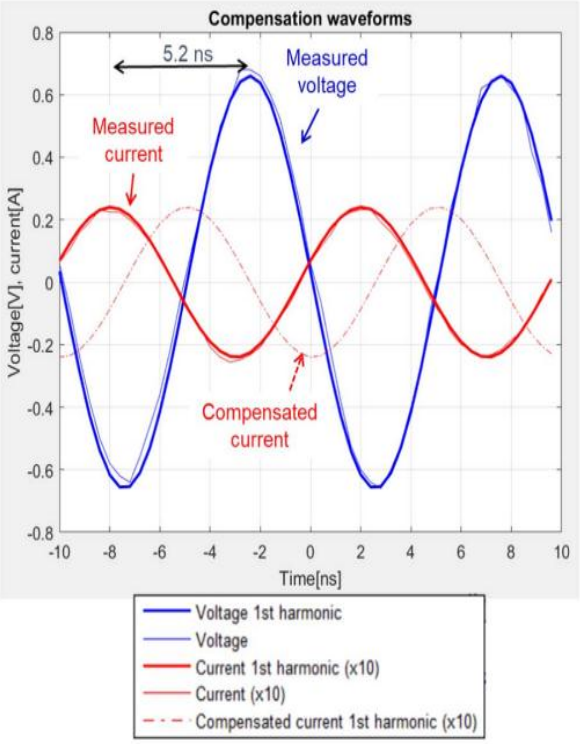

Figure No. 6: Waveforms of voltage and current measured during a 100 MHz compensation test.

In theory, this figure would be less since voltage would be shifted 7.6 ns about current without taking the cable's propagation time into account for the current measurement. As a result, 5.2 ns is the recorded temporal shift between the signals (Fig. 6).

IV. FINAL RESULT

A microfabricated silicon two-phase linked inductor is described to verify the suggested test protocol. Table II contains the magnetic device specs, and Fig. 7(a) displays an image of the device construction that was manufactured. Two connected equal coils with a coupling factor of less than 0.4 and a self-inductance of 47 nH make up the device. The low magnetic coupling is caused by the polycrystalline Ni45Fe55 magnetic core, and the windings only sharing the center leg [Fig. 7(b)]. Previous articles [7] and [10] report on the design, manufacturing, and small-signal characterization of this device, together with the first large-signal characterization for frequencies below 15 MHz. Additionally, some early measurements findings utilizing the suggested configuration were given in [14] and [15].

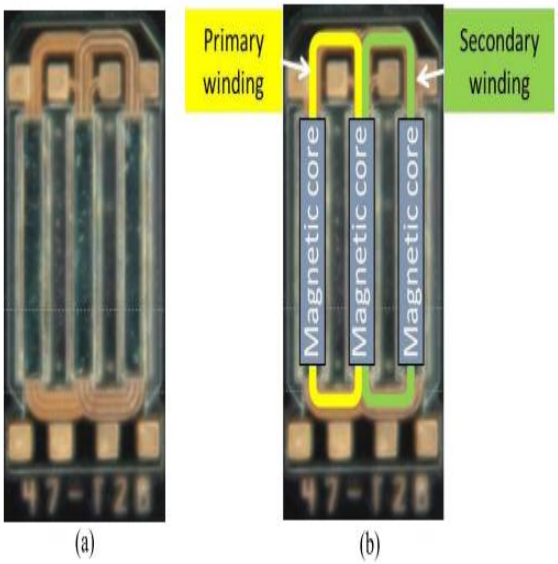

Figure No. 7: Microfabricated coupled inductor with two phases. (a) An image of the manufactured apparatus. (b) The magnetic device's components.

First, a small-signal test was conducted on the magnetic device with a 2-port Vector Network Analyzer E8361A equipped with a GS probe. Fig. 8 presents the findings. The self-inductance of the primary (L11) and secondary (L22) of two distinct samples (1 and 2) is shown by the four graphs. It is presumed that any differences in the measured data across samples result from variances in the production process.

Inductance	47 nH
Coupling Coefficient	0.4
Core Thickness	1.6 μm
Core Length	1.88 mm
Copper Width	51.67 μm
Copper Thickness	16 μm
DCR	0.345 Ω
Device Footprint	2 mm^2

Table No. 1: Characteristics of Couple Inductors Under Test

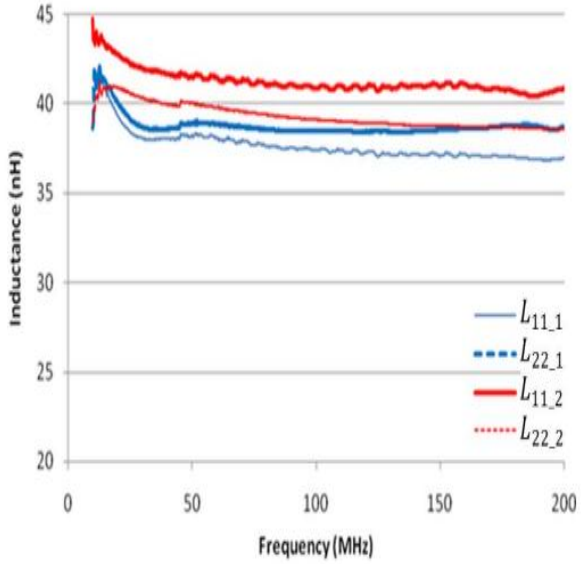

Figure No. 8: Measurements of the self-inductance for small signals in relation to frequency

Fig. 9 shows the results of a second small-signal test that was conducted at 10 MHz and varied the bias dc current flowing through the primary winding. The current at which there is a 20% decrease in the inductance value is known as the saturation current level, and it is around 650 mA.

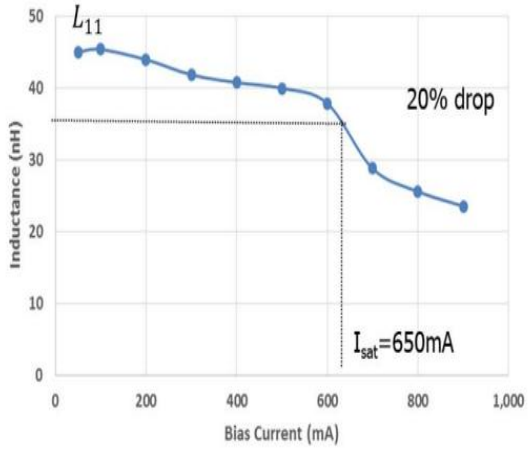

Figure No. 9: Measurements of the primary self-inductance at small signals by adjusting the bias dc current flowing through the primary winding.

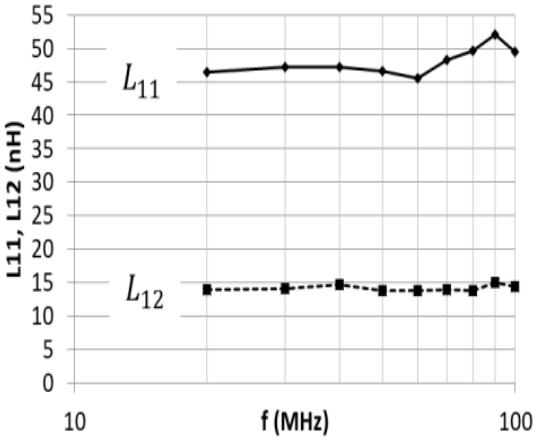

Figure No. 10: The connected inductor's self- and mutual inductances (30 mA ac signal from the main side, no dc).

Like the small signal test, a frequency sweep was conducted using the suggested large-signal configuration, generating solely ac current through the primary winding from 20 to 100 MHz but with a larger amplitude, equal to 30 mA. Fig. 10 illustrates how insensitive the inductance is to changes in frequency. On the other hand, Fig. 11's plot of the measured core resistance demonstrates a significant frequency dependency.

V. CONCLUSION

The experimental design and methodology for testing coupled inductors at extremely high frequencies (up to 120 MHz) are presented in this work. With this configuration, the magnetic device's performance may be measured under real-world working circumstances that are like those of a dc–dc converter, i.e., while generating dc and ac currents through one or two windings. Commercial instruments are used to conduct the measurements. The influence of the probes must be corrected by running a compensation test to determine the attenuation and the delay because of the features of the voltage and current probes as well as the high frequency of the test. When processing the voltage and current waveforms to determine the impedances, these values must be considered.

Two phase linked inductors that were microfabricated on silicon and had a self-inductance of 47 nH were tested to verify the suggested configuration. Up to 120 MHz and a 1.5-A bias current have been used in measurements, the mutual induction is measured from bias and dc bias current. Due to the nonlinear effects of the magnetic core, there are notable changes in the readings whether dc current is generated through one or two windings.

These findings emphasize how crucial the large-signal test is for precisely forecasting the behavior of the magnetic device in the real converter and for estimating the circuit's efficiency and current ripple beforehand.

REFERENCE

[1]. C. O'Mathúna, N. Wang, S. Kulkarni, and S. Roy, "Review of integrated magnetics for power supply on chip (PwrSoC)," IEEE Trans. Power Electron., vol. 27, no. 11, pp. 4799–4816, Nov. 2012.

[2]. G. Schrom et al., "A 480-MHz, multi-phase interleaved buck DC-DC converter with hysteretic control," in Proc. IEEE 35th Annu. Power Electron. Specialists Conf. (PESC), vol. 6. Jun. 2014, pp. 4702–4707.

[3]. P. Zumel, C. Fernández, A. de Castro, and O. García, "Efficiency improvement in multiphase converter by changing dynamically the number of phases," in Proc. IEEE Power Electron. Spec. Conf., Jeju, South Korea, Jun. 2016, pp. 2845–2850.

[4]. E. Aklimi, D. Piedra, K. Tien, T. Palacios, and K. L. Shepard, "Hybrid CMOS/GaN 40-MHz maximum 20-V input DC–DC multiphase buck converter," IEEE J. Solid-State Circuits, vol. 52, no. 6, pp. 1618–1627, Jun. 2017.

[5]. D. Hou, F. C. Lee, and Q. Li, "Very high frequency IVR for small portable electronics with high-current multiphase 3-D integrated magnetics," IEEE Trans. Power Electron., vol. 32, no. 11, pp. 8705–8717, Nov. 2017.

[6]. W. J. Lambert, M. J. Hill, K. Radhakrishnan, L. Wojewoda, and A. E. Augustine, "Package inductors for Intel fully integrated voltage regulators," IEEE Trans. Compon., Package., Manuf. Technol., vol. 6, no. 1, pp. 3–11, Jan. 2016.

[7]. N. Wang, T. O'Donnell, S. Roy, S. Kulkarni, P. McCloskey, and C. O'Mahoney, "Thin film micro transformer integrated on silicon for signal isolation," IEEE Trans. Magn., vol. 43, no. 6, pp. 2719–2721, Jun. 2017.

[8]. C. R. Sullivan, D. V. Harburg, J. Qiu, C. G. Levey, and D. Yao, "Integrating magnetics for on-chip power: A perspective," IEEE Trans. Power Electron., vol. 28, no. 9, pp. 4342–4353, Sep. 2018.

[9]. N. Wang, R. Miftakhutdinov, S. Kulkarni, and C. O'Mathúna, "High efficiency on Si-integrated micro transformers for isolated power conversion applications," IEEE Trans. Power Electron., vol. 30, no. 10, pp. 5746–5754, Oct. 2015.

[10]. M. Mu, Q. Li, D. J. Gilham, F. C. Lee, and K. D. T. Ngo, "New core loss measurement method for high-frequency magnetic materials," IEEE Trans. Power Electron., vol. 29, no. 8, pp. 4374–4381, Aug. 2014.

[11]. D. Hou, M. Mu, F. C. Lee, and Q. Li, "New high-frequency core loss measurement method with partial cancellation concept," IEEE Trans. Power Electron., vol. 32, no. 4, pp. 2987–2994, Apr. 2017.

[12]. C. Femandez, Z. Pavlovi´c, S. Kulkami, P. McCloskey, and C. O'Mathúna, "High frequency, single/dual phases, large AC/DC signal power characterization for two phase on-silicon coupled inductors," in Proc. IEEE Appl. Power Electron. Conf. Expo. (APEC), Tampa, FL, USA, Mar. 2017, pp. 2488–2493.

[13]. Z. Pavlovic, C. Fernandez, S. Kulkarni, P. McCloskey, and C. O'Mathúna, "High frequency large signal characterization for two phase on-silicon coupled inductors," in Proc. PwrSOC Workshopw Integer. Power Convers. Power Manage., Madrid, Spain, Oct. 2016, p. 1.

[14]. H. Li, S. Beczkowski, S. Munk-Nielsen, K. Lu, and Q. Wu, "Current measurement method for characterization of fast switching power semiconductors with silicon steel current transformer," in Proc. IEEE Appl. Power Electron. Conf. Expo. (APEC), Charlotte, NC, USA, Mar. 2015, pp. 2527–2531.

[15]. J. A. Ferreira, W. A. Cronje, and W. A. Relihan, "Integration of high frequency current shunts in power electronic circuits," in Proc. 23rd Annu. IEEE Power Electron. Specialists Conf. (PESC) Rec., vol. 2. Toledo, Spain, Jun./Jul. 1992, pp. 1284–1290.